ELSEVIER

Ceramics International 31 (2005) 641–646

CERAMICS INTERNATIONAL

www.elsevier.com/locate/ceramint

Preparation and characterization of macroporous sol–gel bioglass

Na Li, Qing Jie, Sumin Zhu *, Ruoding Wang

Chinese Academy of Sciences, Shanghai Institute of Ceramics, 1295 Ding-Xi Road, Shanghai 200050, China

Received 3 March 2004; received in revised form 29 March 2004; accepted 24 May 2004
Available online 7 March 2005

Abstract

Sol–gel bioglasses have many advantages comparing to melt-derived bioglasses. 3-D scaffold prepared by sol–gel method is a promising substrate material for bone tissue engineering. But, it is difficult to produce macroporous sol–gel bioglasses with pores larger than 100 μm. In this work, a series of macroporous bioglasses was produced by adding PEG particles into the sol as pore former. The mesoporous texture features of the samples were assessed through a nitrogen sorption technique. The macropore structure was collected by intrusion mercury porosimetry. In vitro tests showed that the samples had good bioactivity. Combining the sol–gel routine with the pore former might be a useful approach for preparation scaffolds with applications to the repair and reconstruction of damaged tissue.
© 2004 Elsevier Ltd and Techna Group S.r.l. All rights reserved.

Keywords: A. Sol–gel processes; B. Porosity; D. Glass; E. Biomedical applications

1. Introduction

Bone regeneration is required in many clinical issues addressed by orthopaedic and dental medicine. The autogeneous bone graft is the gold standard, but host tissue is often scarce and can hardly be modeled to the shape required for successful reconstruction [1]. Then people's attention was transferred to implantation. Although bioactive ceramics have achieved great application successes in bone repairing, their elastic modulus mismatch and stress shielding of human bone cannot fill the longer and longer lifetimes. Tissue engineering provides a new approach for solving these problems. The biomaterials should be the scaffold to assist or enhance the body's own reparative capacity [2].

A scaffold for tissue engineering should provide a template and support tissue growth. An ideal scaffold should be a macroporous material with two important characteristics: the first, an interconnected network with large pores (greater than 100 μm) to enable tissue ingrowth and nutrient delivery to the center of the regenerated tissue; the second, pores in the microporous or mesoporous range to promote cell adhesion, adsorption of biologic metabolites, and resorbability at controlled rates to match that of tissue repair [3].

Bioglasses could elicit a specific biological in vivo response at the interface and attach to the tissues, such as soft tissue and bone, with a strong chemical bond. So they have been widely used for a number of different applications. Certain compositions of bioactive glasses containing SiO_2–CaO–P_2O_5 bond to both soft and hard tissue without an intervening fibrous layer. Results of in vivo implantation show that these compositions produce no local or systemic toxicity, no inflammation, and no foreign-body response [3]. Recent research shows that there is genetic control of the cellular response of osteoblasts to bioactive glasses [4].

Compositions of sol–gel-derived bioactive glasses were used because they exhibit high specific area, high osteoconductive properties, and also a significant degradability [5]. Furthermore, bioglasses prepared via sol–gel method always have an interconnected mesoporous structure, with the pores about 5–10 nm in diameter. Macroporous sol–gel bioglass with pores larger than 100 μm and that about 5–10 nm simultaneously would be an ideal scaffold material.

It is very difficult to produce macroporous sol–gel glasses with a pore size larger than 100 μm because of the great shrinkage during sol–gel processing. In the last few years, the successful applications of high relative humidity in the

* Corresponding author. Tel.: +86 21 52412058; fax: +86 21 52413903.
E-mail address: smzhu@mail.sic.ac.cn (S. Zhu).

0272-8842/$30.00 © 2004 Elsevier Ltd and Techna Group S.r.l. All rights reserved.
doi:10.1016/j.ceramint.2004.05.011

Table 1
The mesoporous structure of 58S and the macroporous specimens prepared in this work

Designation	PEG particles size used (μm)	Particle/sol ratio (% g/ml)	Specific surface area (m^2/g)	Pore volume (cm^3/g)	Mean pore diameter (nm)
58S	–	–	276	0.29	3.4
PEG-S-0.8	150–200	4	325	0.22	4.2
PEG-M-0.8	200–315	4	261	0.09	4.3
PEG-M-1.0	200–315	5	284	0.35	4.8

gel drying [6] have made it possible to prepare macroporous sol–gel with pore former. In this study, we try to prepare macroporous sol–gel bioglasses using granular polyethylene glycol (PEG) as pore former.

2. Materials and methods

2.1. Sample preparation

The composition of 58S bioglass is: $SiO_2$58 wt.%, CaO 33 wt.%, $P_2O_5$9 wt.%. The procedures were similar to those used by Zhong and Greenspan [7]. The 58S sol was prepared by mixing distilled water, HNO_3, tetraethoxysilane, triethylphosphate and calcium nitrate tetra-hydrate in order. The granular PEG (molecular weight 10,000) was used as pore former. The raw material was ground and sieved before experiment and two size ranges (150–200 μm and 200–315 μm) were chosen. After the sols were aged in a drying oven at 60 °C to reach the high enough viscosity, the prepared PEG particles were added into them with strong stirring for mixing uniformly. Then the mixture was poured into molds to gel. In this work, two particle/sol ratios (weight of PEG particles/volume of sol = 0.8 g/20 ml and 1.0 g/20 ml) were used. The obtained specimens were listed in Table 1.

After aging for one day, the gels were moved into drying vessels. They were dried in an environment containing 50/50% mixture of water/ethanol, the temperature was raised to 120 °C slowly and kept for 48 h. Finally the dried gels were then heated to 700 °C for stabilization.

2.2. Characterization of the samples

The specific surface area and the porosity were determined by nitrogen adsorption technique (Tristar 3000, Micromeritics, USA). The macroporous network was analyzed using mercury intrusion porosimetery (Poresizer 9320, Micromeritics, USA). Large and total pore results are measured from pressure 0 to 25 psia (the macro-results) and 0-30000 psia (the total results) respectively.

2.3. In vitro test

Simulated body fluids (SBF) soaking was used to test the in vitro bioactivity of P-S-0.8 samples. The samples were immersed in SBF [8] with ion concentrations nearly equal to human blood plasma at static conditions with a surface area to solution volume ratio of 15.2×10^{-6} m. The substrate surface area was calculated from the total pore area measured by intrusion mercury porosimetry. The reaction time periods were 1, 6, 24 h and 3, 5, 7, 14 days. After each time period, the samples were withdrawn from the solution and washed with distilled water gently, dried and saved for test. Then X-ray diffraction (XRD, Model D/max 2550V, Rigaku, Tokyo, Japan) was employed to investigate the apatite layer formation. SEM-EDS (JSM 6700F, JEOL, Japan) was used to observe HCA growth on the disc surfaces. All the reacted solutions were saved for Inductively Coupled Plasma atomic emission spectroscopy (ICP-AES; Varian Co., USA) analysis of Ca, P and Si to measure ionic release rates for these materials. The pH-values were determined by an electrolyte-type pH meter (Jingke Leici Co., Shanghai, China).

3. Results and discussion

Flawless monolithic macroporous sol–gel bioglasses were produced with different pore sizes and porosities. All the samples showed satisfactory handle resistance.

3.1. Characterization of the glasses

Table 1 lists the BET data of the samples, which show their pore texture features. The macroporous samples exhibited a mesoporous network (average diameter of 4.2–4.8 nm) with a high surface area of 261–325 m^2/g.

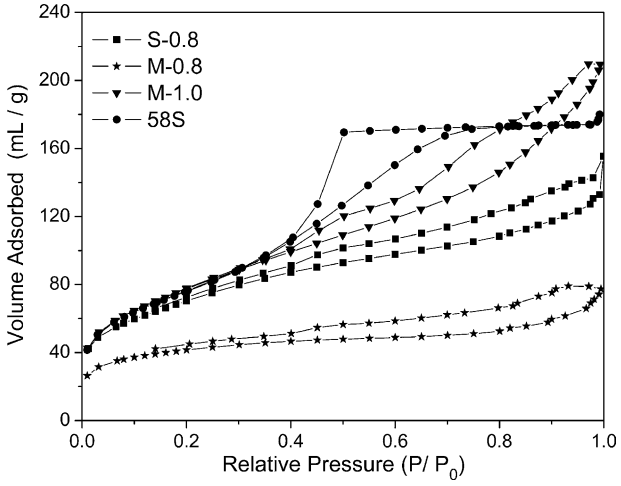

Fig. 1. Nitrogen adsorption–desorption isotherm plots of obtained samples.

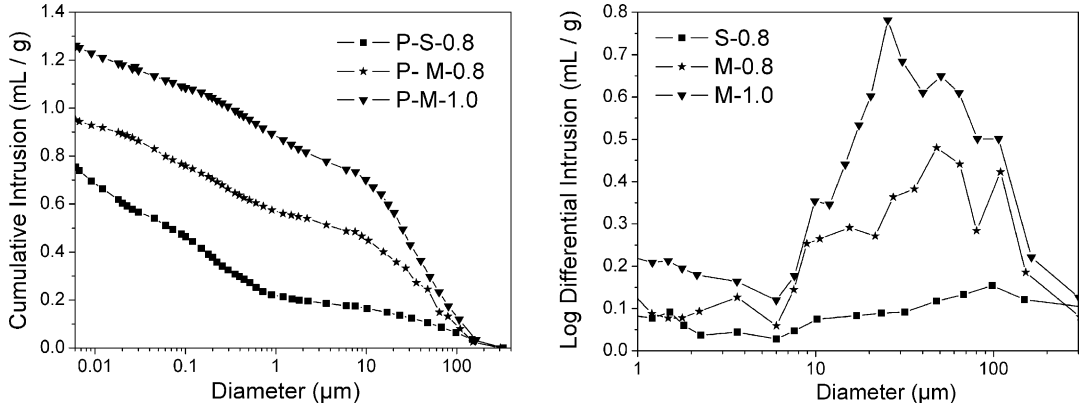

Fig. 2. Mercury porosimetry curves for macroporous bioglass.

Comparing to 58S, the macroporous samples have larger average mesopore diameters. Fig. 1 shows the nitrogen sorption isotherms plots of these samples. The 58S exhibited type H2 hysteresis loops between adsorption and desorption modes, according to BDDT classification, while the macroporous samples yield H3 hysteresis loops which is indicative of mesoporous materials [9]. Adding PEG particles affected the texture a little but maintained the mesoporous feature. Due to the mesoporous texture, the materials exhibit a high specific surface area, which enhances ion release from the surface and therefore the bioactivity of the samples [1].

Fig. 2 compares the pore volumes and macropore-size distribution of the specimens measured by mercury intrusion porosimetry. Mercury intrusion porosimetry is usually used to measure the smaller pores, corresponding to the connecting contact areas or necks between much larger pores created by PEG particles [3]. So the peaks of plots in these pictures are not accurately corresponding to the real values. But we could still see the influence of PEG volume and particle size on the pore-size distribution in these pictures. The larger PEG volume resulted in a higher intrusion volume. And the larger PEG particle size, the larger average pore diameter. The pore diameter distribute around 1–10 μm may come from the PEG dissolved into sol during the mixing procedure.

The results of Hg porosimetry (listed in Table 2) demonstrate that the samples are highly porous with porosities of 60–70%. As mercury intrusion porosimetry accounts only for pores with sizes 250 μm and smaller, we assumed that the true porosity may even be higher. The high porosity presented by these materials can provide diffusion pathways and ample room for protein adsorption and protein delivery [1].

Table 2
Data of average pore size and pore volume of the macroporous specimens measured by mercury intrusion porosimetry

Designation	Average pore diameter (nm)	Pore volume (cm^3/g)	Macroporosity (%)	Total porosity (%)
PEG-S-0.8	39	0.754	14.0	60.3
PEG-M-0.8	100	0.950	33.1	64.5
PEG-M-1.0	114	1.261	41.3	70.8

The nitrogen sorption results combined with mercury porosimetry results indicate that the samples are 3D hierarchical structures of a macropore (10–200 μm) network in a matrix containing mesopores (2–50 nm). It was demonstrated that the porosity and the macropore diameter could be controlled by altering the volume and size of pore former, so we can control the tissue ingrowth rates. Different texture of sol–gel materials could be obtained by changing the sol–gel processing or treatment parameters. Thus degradation rates and surface chemical binding sites can be controlled for sol–gel bioglasses.

3.2. Bioactivity assays in SBF

3.2.1. Changes in the surface of the glasses

The X-ray diffraction analysis results of the glass P-S-0.8 are shown in Fig. 3. In the untreated pattern, 58S sample almost takes amorphous state indicative of the internal disorder and glassy nature of these materials [10]. The substance formed on glasses became detectable after 1 day immersion in SBF, new peaks (at $2\theta\sim$ 32°, 26°) were

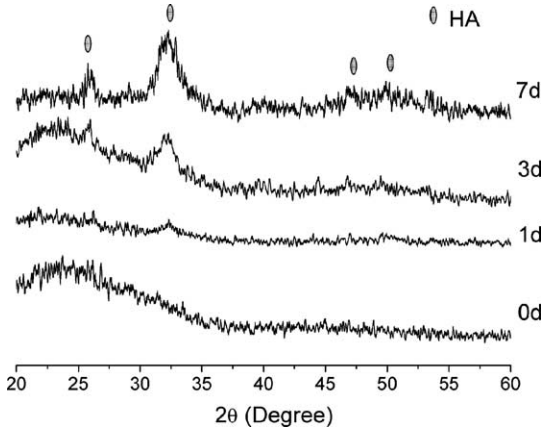

Fig. 3. XRD patterns of glasses before and after soaking in SBF for 1, 3 and 7 days.

assigned to be (2 1 1), (0 0 2) apatite according to the standard JCPDS cards (09-0432). After 3 days immersion, the two peaks were intensified and the other peaks of apatite at 40°, 46°, 49° also appeared. After 7 days immersion all the peaks became more apparently. The widen diffraction peak at 2θ ranging from 30° to 34°, which should be distinguished the (2 1 1), (1 1 2) and (3 0 0) planes for well-crystallized hydroxyapatite, indicates the poor crystallinity of the apatite [11].

Fig. 4 is the images observed by FESEM, which show HA formation on the plane surfaces and in the large pore of P-S-0.8 samples, and the unreacted sample was provided here for comparison. These images corroborated the XRD results. It should be noted that there were already a lot of spherical-shaped HA particles aggregation appeared in the large pores after immersion in SBF for one day, however there was only a little and small HA particles dispersed on the plane surface. Although the specific surface area is very high, a large fraction of the internal surface might not have been readily accessible to the SBF solution because of diffusion limitations and deposition of HA at the surface. For the large pores with a diameter several hundred micrometers, it allow the SBF to infiltrate the material freely and permitted more efficient transport of ions to and from the reactive

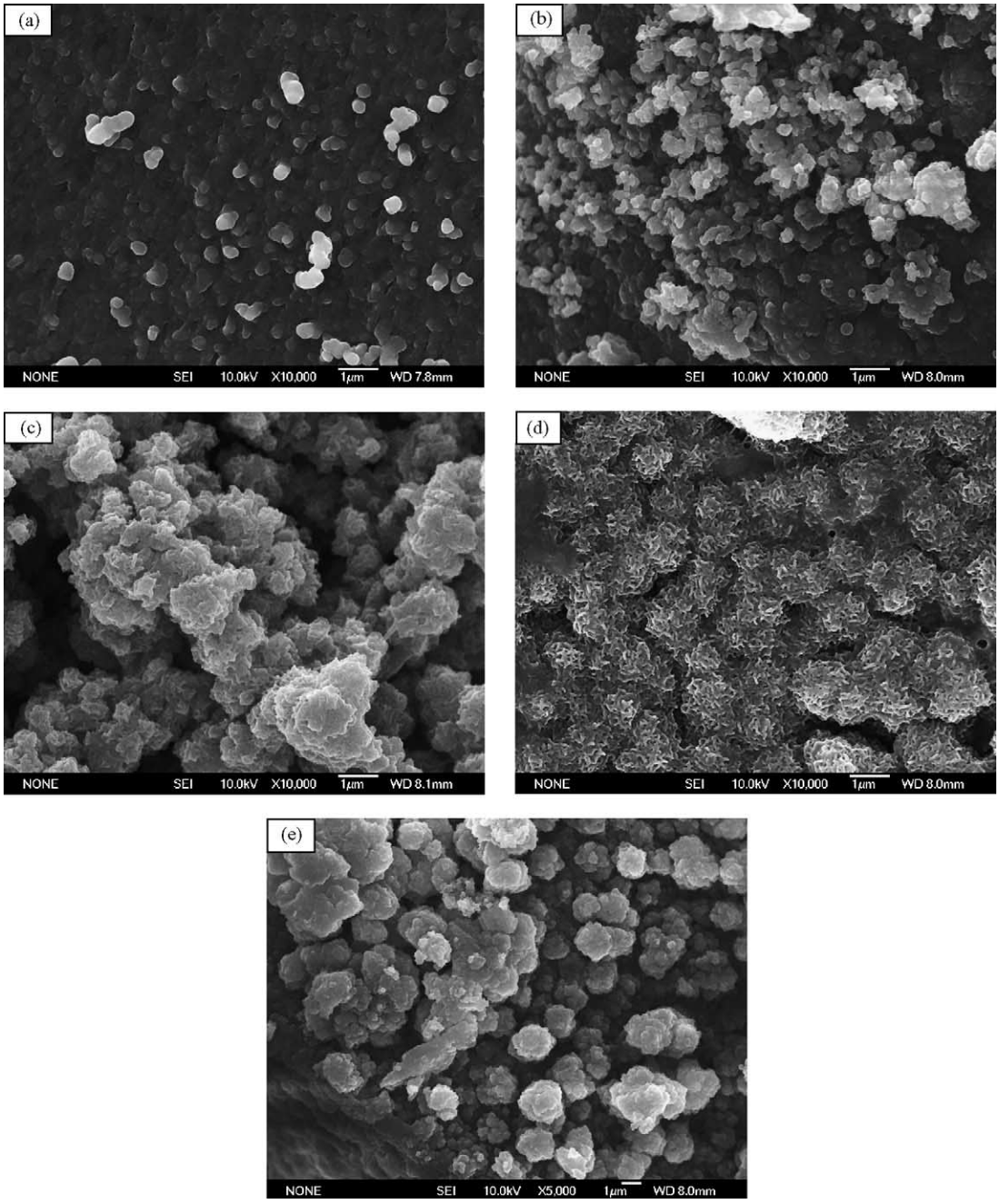

Fig. 4. SEM micrographs of PEG-S-0.8 samples before and after in vitro test.

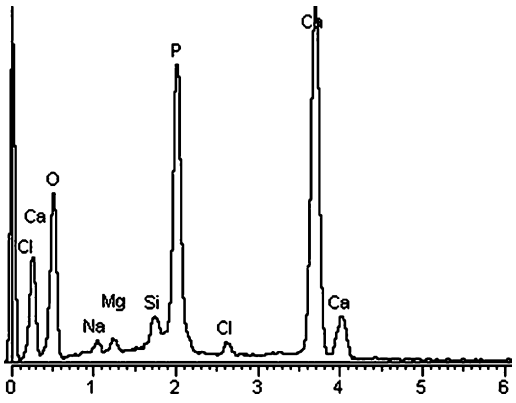

Fig. 5. EDS spectra of sample immersed for 7days.

surface, resulting in the better activity of the large pores wall toward mineralization. After 3 day's immersion the large pores and the surface had almost been covered by this sort of aggregated HA particles. As can be observed, the spherical particles are formed by numerous needles and the size of such particles is about 1–4 μm. Seven days later, HA had completely covered the sample surface and the Needle-shape appeared more clearly. The EDS results of 7 days immersion (Fig. 5) indicate that the precipitated layers are composed of Ca and P with a Ca/P atomic ratio of 1.50 less than 1.67 (the theoretical value Ca/P ratio of apatite), and contain a small quantity of Mg [12].

3.2.2. Changes in SBF composition

Fig. 6 shows the variations of Ca, Si and P concentration as well as pH values in the SBF solution for various periods. The results indicate that the glasses leach silicon, while calcium and phosphate precipitate on their surface [13]. The Si concentration continued to increase with the prolonged soaking time. On the other hand, the P content decreased continually because phosphorus dissolved slowly from the substrate structure in SBF. The Ca^{2+} concentration is controlled by both the release of Ca^{2+} from the substrate and the formation of phosphate or HCA. In the first 24 h the Ca^{2+} concentration increased drastically, which means the rapid calcium dissolution. However after a maximum immersion at 24 h, the Ca^{2+} concentration gradually decreased up to 7 days, and a little rise to 14 days. The decrease in the Ca^{2+} concentration in SBF is attributed to the rapid growth of the apatite nuclei formed on surface of the glasses that overcame the release rate of calcium ions to the solution [14]. The little rise of Ca^{2+} concentration in SBF can be explained by the implement of the dense apatite layer, which slowed the apatite growth so that the dissolution rate exceeding the depletion Ca^{2+} rate. The glasses give rise to a marked P deposit in the first 3 days, and then the deposit rate become slow indicating that HA growth slowed down [15]. Simultaneously the Si release rate decreased remarkably after 3 days of assay, and then decreased gradually with the longer soaking time. It can be summarized that the apatite growth rate increased to maximum at 3 days assay then decreased more and more.

The pH varied corresponding to Ca^{2+} concentration variations. The reason is that Ca^{2+} in the glass exchanged with H^+ or H_3O^+ in the SBF, and then a SiO_2 rich layer formed on the glass surface.

4. Conclusion

Different sizes of macroporous sol–gel bioglasses were obtained by adding granular PEG into the 58S sol as pore former. Using this method, it is easy to control pore diameter and volume by changing the size range and volume of PEG particles. The large pore size ranging from 100 to 300 μm is not only large enough for cell's attachment, but also suitable for tissues and blood vessels to grow in. The in-vitro tests indicated that these materials had good bioactivity; in addition, the macroporous structure did play an important role in the apatite formation procedure. Mesopores about 4nm also characterize these sol–gel materials. The mesoporous texture can promote the bioactivity and the degradation rate. All of these results suggest that these sol–gel bioglasses are new materials with the potential to fulfill the demands of bone tissue engineering and enhance tissue regeneration.

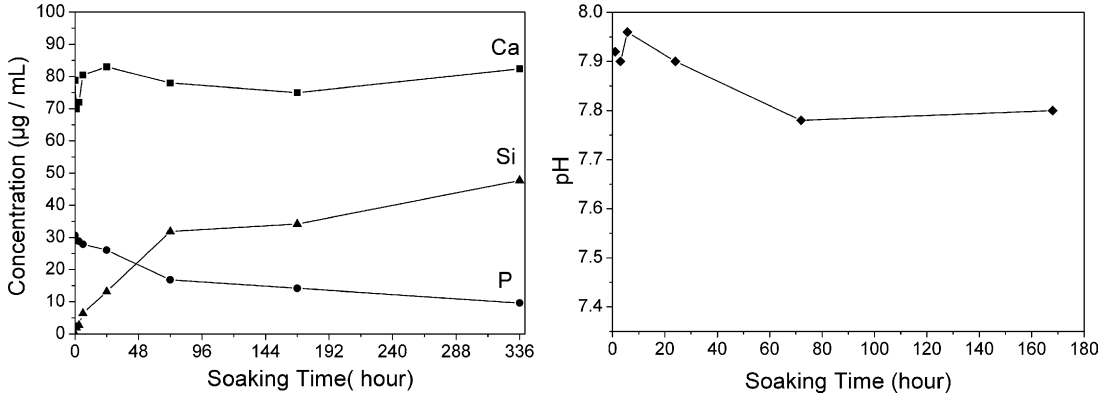

Fig. 6. Ca, P, Si concentration and pH change with soaking time in SBF.

Reference

[1] R.F.S. Lenza, W.L. Vasconcelos, J.R. Jones, L.L. Hench, Surface-modified 3D scaffolds for tissue engineering, J. Mater. Sci.: Mater. Med. 13 (2002) 837–842.

[2] J.R. Jones, L.L. Hench, Biomedical materials for new millennium: perspective on the future, Mater. Sci. Tech. 17 (2001) 891–900.

[3] P. Sepulveda, J.R. Jones, L.L. Hench, Bioactive sol–gel foams for tissue repair, J. Biomed. Mater. Res. 59 (2002) 340–348.

[4] L.L. Hench, J.M. Polak, Third-generation biomedical materials, Science 295 (2002) 1014–1017.

[5] P. Saravanapavan, L.L. Hench, Low-temperature synthesis, structure, and bioactivity of gel-derived glasses in the binary $CaO–SiO_2$ system, J. Biomed. Mater. Res. 54 (2001) 608–618.

[6] J.P. Zhong, D.C. Greenspan, Porous sol–gel bioglass from near-equilibrium drying, in: Sedel, Rey (Eds.), Bioceramics, vol. 10, Elsevier Science, New York, 1997, pp. 265–268.

[7] J.P. Zhong, D.C. Greenspan, Processing and properties of sol–gel bioactive glasses, J. Biomed. Mater. Res. 53 (2000) 694–701.

[8] T. Kokubo, et al. Solution able to reproduce in vivo surface-structure changes in bioactive glass-ceramic A-W, J. Biomed. Mater. Res. 24 (1990) 721–734.

[9] N.J. Coleman, L.L. Hench, A gel-derived mesoporous silica reference material for surface analysis by gas sorption. Textural features, Ceram. Int. 26 (2000) 171–178.

[10] J. Pérez-Pariente, F. Balas, J. Román, A.J. Salinas, M. Vallet-Regí, Influence of composition and surface characteristics on the in vitro bioactivity of $SiO_2–CaO–P_2O_5–MgO$ sol–gel glasses, J. Biomed. Mater. Res. 61 (2002) 524–532.

[11] P. Li, I. Kangasniemi, K. de Groot, T. Kokubo, Bonelike hydroxyapatite induction by a gel-derived titania on a titanium substrate, J. Am. Ceram. Soc. 77 (5) (1994) 1307–1312.

[12] N. Olmo, A.I. Martin, A.J. Salinas, Bioactive sol–gel glasses with and without hydroxycarbonate apatite layer as substrates for osteoblast cell adhesion and proliferation, Biomaterials 24 (2003) 3383–3393.

[13] D.C. Greenspan, J.P. Zhong, X.F. Chen, G.P. LaTorre, The evaluation of degradability of melt and sol–gel derived bioglass in vitro, Bioceramics 10 (1997) 391–394.

[14] A. Martinez, I. Izquierdo-Barba, M. Vallet-Regi, Bioactivity of a $CaO–SiO_2$ binary glasses system, Chem. Mater. 12 (2000) 3080–3088.

[15] H. Yan, K. Zhang, C.F. Blanford, L.F. Francis, A. Stein, In vitro hydroxycarbonate apatite mineralization of $CaO–SiO_2$ sol–gel glasses with a three-dimensionally ordered macroporous structure, Chem. Mater. 13 (2001) 1374–1382.